Preprints.org

Article

Not peer-reviewed version

Optical Biosensor Based on Porous Silicon and Tamm Plasmon Polariton for Detection of CagA Antigen of *Helicobacter Pylori*

Guoguang Rong , Alexey Kavokin , Mohamad Sawan *

Posted Date: 31 January 2024

doi: 10.20944/preprints202401.2192.v1

Keywords: Optical Biosensor; Tamm Plasmon Polariton; Porous Silicon; CagA antigen; *Helicobacter Pylori*; High Sensitivity; Specificity; Disgnostics

Preprints.org is a free multidiscipline platform providing preprint service that is dedicated to making early versions of research outputs permanently available and citable. Preprints posted at Preprints.org appear in Web of Science, Crossref, Google Scholar, Scilit, Europe PMC.

Copyright: This is an open access article distributed under the Creative Commons Attribution License which permits unrestricted use, distribution, and reproduction in any medium, provided the original work is properly cited.

Preprints.org (www.preprints.org) | NOT PEER-REVIEWED | Posted: 31 January 2024 doi:10.20944/preprints202401.2192.v1

Disclaimer/Publisher's Note: The statements, opinions, and data contained in all publications are solely those of the individual author(s) and contributor(s) and not of MDPI and/or the editor(s). MDPI and/or the editor(s) disclaim responsibility for any injury to people or property resulting from any ideas, methods, instructions, or products referred to in the content.

Article

Optical Biosensor Based on Porous Silicon and Tamm Plasmon Polariton for Detection of CagA Antigen of *Helicobacter Pylori*

Guoguang Rong [1], Alexey Kavokin [2] and Mohamad Sawan [1,*]

[1] CenBRAIN Neurotech Center of Excellence, School of Engineering, Westlake University, Hangzhou 310030, China

[2] The International Center for Polaritonics, School of Sciences, Westlake University, Hangzhou 310030, China

* Correspondence: sawan@westlake.edu.cn

Abstract: Helicobacter Pylori (H. Pylori) is a common pathogen with high prevalence of infection in human populations. Diagnosis of H. Pylori infection is critical for its treatment, eradication, and prognosis. Biosensors have been demonstrated to be powerful for rapid onsite detection of pathogens, particularly for point-of-care test (POCT) scenarios. In this work, we propose a novel optical biosensor, based on nanomaterial porous silicon (PSi) and photonic surface state Tamm Plasmon Polariton (TPP), for detection of cytotoxin-associated antigen A (CagA) antigen of H. Pylori bacterium. We fabricated the PSi TPP biosensor, analysed its optical characteristics and demonstrated through experiments towards sensing of CagA antigen, that TPP biosensor has sensitivity of 100 pm/(ng/ml), limit of detection of 0.01 ng/ml, and specificity in terms of positive-to-negative ratio of more than six. From these performance factors, it can be concluded that TPP biosensor can serve as an effective tool for diagnosis of H. Pylori infection, either in analytical labs or in POCT applications.

Keywords: optical biosensor; Tamm Plasmon Polariton; porous silicon; CagA antigen; helicobacter pylori; high sensitivity; specificity; disgnostics

Introduction

Helicobacter pylori is a very common pathogenic bacterium. According to statistics, more than half of the world population are infected with Helicobacter pylori [1]. Helicobacter pylori is a spiral shaped bacterium, abbreviated as H. Pylori, that can infect human stomach. H. Pylori exists in various regions of the stomach and duodenum, with strong activity and reproductive ability, posing a great threat to human health. H. Pylori is mainly transmitted through oral-oral or fecal-oral routes of transmission, causing nausea, acid reflux, belching, upper abdominal discomfort, decreased appetite, and bad breath [2]. The diagnostic of H. Pylori infection is very important for infection diagnosis, controlling its activity, eradication confirmation, and health restoration [3].

Depending on whether endoscopy is used, diagnostic techniques for H. Pylori can be classified into two main categories: non-invasive and invasive techniques. Non-invasive techniques include urea breath test [4], stool antigen test [5], serological test [6] and biosensing [7–9]. Invasive techniques include endoscopy [10], histology [11], culturing [12], rapid urea test [13], and polymerase chain reaction [14]. We summarize and compare in Table 1 the currently available diagnostic techniques for H. Pylori reported in academic literature. Also, included in Table 1, the biosensor technique, which is discussed in the following.

Table 1. Comparison of Different H. Pylori Detection Techniques.

Detection Techniques		Pros	Cons
Non-invasive test methods	Serological test [6]	No side effects on patients	Positive results may not mean persistent infection

© 2024 by the author(s). Distributed under a Creative Commons CC BY license.

Preprints.org (www.preprints.org) | NOT PEER-REVIEWED | Posted: 31 January 2024 doi:10.20944/preprints202401.2192.v1

(Endoscopy not required)	Stool antigen test [5]	Easy operation	Fecal sample handling may affect results
	Urea breath test [4]	Easy operation	Drugs taken by patients may impact accuracy
	Biosensors [7–9]	Easy operation, high sensitivity	Specificity may be affected by interferents in samples
Invasive test methods (Endoscopy required)	Endoscopy [10]	Gastric pathology observation available	Accuracy may vary drastically depending on operator experiences
	Culturing [12]	Highly specific due to controlled culturing conditions	Long turnaround time and vulnerability of results to culturing conditions
	Histological test [11]	High sensitivity and specificity	Accuracy may vary drastically depending on operator experiences
	Rapid urease test [13]	Rapid and easy to operate	Bacterium may not be present in biopsy
	Polymerase chain reaction (PCR) [14]	Accurate and high throughput capability	Need clean environment, samples may contain PCR blockers

Authors have demonstrated that biosensors are powerful tools for rapid onsite detection of pathogens, antigens, and biomarkers. Due to their high sensitivity, good specificity, ease of operation, and low cost, biosensors have been used for diagnosis of H. Pylori infection as well. For example, an electrochemical biosensor was used to detect DNA of H. Pylori with limit of detection (LOD) of 0.06 μg/ml and dynamic range of 0.72-7.92 μg/ml [7]. In another work, a piezoelectric biosensor has been used to serologically determine H. Pylori infection through the detection of IgG antibodies with biosensor signal amplification by a secondary antibody binding with IgG [6]. Moreover, an optical biosensor to detect urease gene of H. Pylori by gold nanoparticle labeled probe with LOD of 0.5 nM has also been reported [8]. In addition, colorimetric detection of H. Pylori through natural pH indicators, together with image processing to achieve LOD of 10 CFU/ml, has been demonstrated [9].

Among these available biosensing techniques, optical biosensors have the advantages of high sensitivity, good specificity, easy operation, fast response, portability, and compatibility with optoelectronic integration. To illustrate the advantages, optical biosensors based on waveguides [15], ring resonators [16], resonant microcavities [17], photonic crystals [18], optic fibers [19], Surface Plasmon Resonance (SPR) [20], Localized Surface Plasmon Resonance (LSPR) [21], and Surface Enhanced Raman Spectroscopy (SERS) [22], have been proposed as effective detectors of various kinds of bio species, such as and biomarkers, proteins, DNAs, virus, bacterium, and cells. On the other hand, from the material perspective of biosensing technology, porous silicon (PSi) is a versatile nanoscale material for biosensing applications. It has high surface area for biomolecular immobilization, CMOS-compatible fabrication process for integration with electronics or optoelectronics, and facile biofunctionalization approaches based on Si/SiO_2 interface. Porous silicon based optical devices, such as optical waveguide [15], resonant microcavity [17], photonic crystal [23], and Tamm Plasmon Polariton heterostructure [24–26] have all been demonstrated to be efficient biosensing platforms.

Preprints.org (www.preprints.org) | NOT PEER-REVIEWED | Posted: 31 January 2024 doi:10.20944/preprints202401.2192.v1

We have previously proposed a novel optical biosensor based on the nanophotonic phenomenon of an interface optical resonant state-Tamm Plasmon Polariton (TPP) [24–26]. Porous silicon was used to construct a Distributed Bragg Reflector. Gold thin metal film deposited on top of the porous silicon Distributed Bragg Reflector allows the formation of a Tamm Plasmon Polariton resonant device. The gold material serves as a plasmonic or epsilon-near-zero material required to sustain the Tamm Plasmon Polariton mode [27,28]. Signal interrogation of the Tamm Plasmon Polariton optical biosensor was based on the reflection spectroscopy. Machine learning techniques can also be employed to process the optical signals to get reliable detection results [29]. For applications, we have demonstrated the detection of SARS-CoV-2 virus with the porous silicon Tamm Plasmon Polariton optical biosensor. We have also demonstrated detection of nucleocapsid protein of SARS-CoV-2 virus with the PSi TPP optical biosensor.

In this work, based on our previous related research on Tamm Plasmon Polariton based biosensors with porous silicon material [24–26], we propose that the optical PSi TPP biosensor can be used for CagA antigen detection to diagnose H. Pylori infection. PSi TPP biosensor has been demonstrated to have a high sensitivity and a good specificity. It is also compatible with CMOS (Complementary Metal Oxide Semiconductor) fabrication processes, promising low-cost mass production and integration with electronics or optoelectronics. On the other hand, after considering many antigen targets for detection, we found that among the many virulent factors associated with H. Pylori bacterium, such as CagA (Cytotoxin-associated antigen A), VacA (Vacuolating cytotoxin) and BabA (blood group antigen binding adhesin), CagA virulent factor is very important for H. Pylori diagnosis since it has been reported that CagA positive patients may be related to more severe gastritis [30], and that they may even have more tendency towards development of cancer [31] than CagA negative patients.

The detection of CagA antigen with PSi TPP biosensor is based on the interaction of electromagnetic energy confined by TPP resonant mode with biomolecules, such as CagA antigen and antibody. The specific detection of CagA antigen derives from the specific capturing of CagA antigen by CagA antibody physically immobilized on TPP energy confinement region. By optimizing the PSi TPP device structure through temporal critical coupling condition [28], strongest field confinement of TPP resonant mode can be obtained. Therefore, the highest sensitivity of the PSi TPP biosensor can be obtained due to maximized interaction between biomolecules and electrical field. The immobilization strategy of the specific CagA antibodies also plays an important role in the sensitivity and specificity performances of the PSi TPP biosensor. Based on our previous experiences with SARS-CoV-2 N-protein detection, we also developed the immobilization strategy and protocol applicable for CagA antibodies conjugated with PSi TPP biosensor. All these works are intended for highly sensitive and specific PSi TPP biosensor for detection of CagA antigen towards H. Pylori diagnosis.

Materials and Methods

The porous silicon-based TPP device under study is based on the porous silicon Distributed Bragg Reflector (DBR). First, single crystalline silicon wafer (6-inch diameter, Boron doped P-type, 0.01-0.02 Ω·cm resistivity, <100> crystal orientation, ~700 μm thickness, single or double side polished) was soaked in 5% aqueous hydrofluoric acid (HF) solution for 5 minutes to remove the native oxide of approximately 20 nm on top of silicon wafer. Then porous silicon DBR was fabricated by electrochemical anodization of the polished side of the single crystalline silicon wafer in 15% aqueous ethanoic hydrofluoric acid (HF) solution (3:7 v/v of 50% aqueous HF and 99% ethanol). During electrochemical anodization, a platinum wire is in contact with HF and serves as the cathode, while an aluminum plate is in contact with the other side of the silicon wafer (either polished or etched) and serves as the anode. The electrochemical anodization conditions and the resulting structural parameters of porous silicon can be found in Table 2 [24]. The resulting porous silicon material has approximately cylindrical pores with effective circular cross section of about 20-30 nm in pore diameter.

Preprints.org (www.preprints.org) | NOT PEER-REVIEWED | Posted: 31 January 2024 doi:10.20944/preprints202401.2192.v1

Table 2. Porous silicon electrochemical anodization conditions and optical parameters of the resulting porous silicon material.

Porous Silicon Layer	Current Density	Anodization Time	Porosity of Layer	Optical Refractive Index	Thickness of Layer
Low Porosity (LP PSi)	5 mA/cm^2	20 seconds	52%	2.08	100 nm
High Porosity (HP PSi)	48 mA/cm^2	6 seconds	76%	1.46	150 nm

After electrochemical anodization, the porous silicon DBR was thermally oxidized under 800°C in ambient atmosphere for 30 minutes to convert Si-OH groups into more stable Si-O groups. The oxidation process can also make porous silicon more hydrophilic to facilitate aqueous solution infiltration into the nanoscale pores of porous silicon.

Afterwards, gold thin film of approximately 30 nm thickness was deposited on oxidized porous silicon DBR through magnetic controlled sputtering. The gold thin film serves as epsilon-near-zero material in TPP device structure [27]. Then the 6-inch wafer with TPP device fabricated on top was cut into 6mm×6mm chips with a dice saw. Each chip is a TPP device that can serve as a PSi TPP biosensor after biofunctionalization with specific antibodies, binding proteins, or aptamers.

Finally, the TPP chip was biofunctionalized through covalent bond immobilization strategy. In general, the surface of the chip is modified with a polycarboxylation reagent, and then the antibody is immobilized using covalent conjugation method. Table 3 describes the biofunctionalization procedure of PSi TPP biosensor in more details.

Table 3. Biofunctionalization procedure of the PSi TPP biosensor for CagA detection.

No	Step Name	Step Operation
1	Chip cleaning	Clean the surface of the chip separately with anhydrous ethanol and ultrapure water, blow dry the water, and set aside.
2	Carboxyla-tion modification	Dilute the polycarboxylation reagent (Xlement Cat. No. G40005) to 100μM working concentration with ultrapure water, take an appropriate amount of carboxylation reagent and add it to the surface of the chip. Leave it at 4°C overnight or 37°C for 4 hours.
3	Activation of functional groups on surface of biosensors	Wash the carboxylated modified chip three times with ultrapure water and blow dry the moisture. Prepare the experimental chip card following standard operating procedures and connect it to the corresponding flow interface in sequence. Prepare an activation reagent solution with a final concentration of 10 mM using 100 mM activation buffer solution (Xlement Cat. No. S20028), and inject 100 μl activation reagent (prepare when need to use) into the chip with a flow rate of 10 μl/min, Running buffer is the activation buffer.
4	Preparation of immobiliza-tion antibody solution	Prepare solution of capture antibodies against CagA antigen of *Helicobacter Pylori* and dilute with a coupling buffer solution (Xlement Cat. No. S20029) to 15μg/ml concentration for later use.
5	Chip conjugation with antibody	Take an appropriate amount of capture antibody (CagA antibody) solution and add it to the surface of the chip. Inject 100 μl the capture antibody solution into the chip at a flow rate of 10 μl/min. Running buffer is the conjugation buffer.
6	Sealing	Take an appropriate amount of sealing buffer solution (Xlement Cat. No. G30004) and add it to the surface of the chip. Inject 100 μl sealing buffer solution into the chip with a flow rate of 10 μ l/min, the Running buffer is the sealing buffer.

Preprints.org (www.preprints.org) | NOT PEER-REVIEWED | Posted: 31 January 2024 doi:10.20944/preprints202401.2192.v1

7	Storage	The biosensors can be stored for 3-5 days under 37°C, two months under 25°C, and 6 months under 2-8°C.
8	Biosensing	Restore the biosensors to room temperature of 25-27°C. Drop 20 µl of CagA antigen solution in varying concentrations in PBS buffer on biosensor surface. Put on cover glass and take spectral measurement with fiber spectrometer.

The optical characterization of the PSi TPP biosensor is based on reflection spectroscopy which is a commonly used technique in optics. The optical measurement setup is shown in Figure 1. A white light source provides the incident light. The incident light is guided by six circumferential fibers of a Y-shape fiber bundle and impinges on the PSi TPP biosensor surface with a circular shaped beam spot of approximately 1 mm in diameter. The light reflected from the PSi TPP biosensor surface is collected by the central fiber of the Y-shape fiber bundle and then guided towards the spectrometer of pm-resolution for spectral analysis. Visible light of 400-800 nm in wavelength is used to interrogate the reflection spectrum of the PSi TPP biosensor, which is light intensity as a function of wavelength $I_{Original}(\lambda)$. For correction of light source emission spectrum, silver mirror was used as a reference to get $I_{Silver}(\lambda)$.

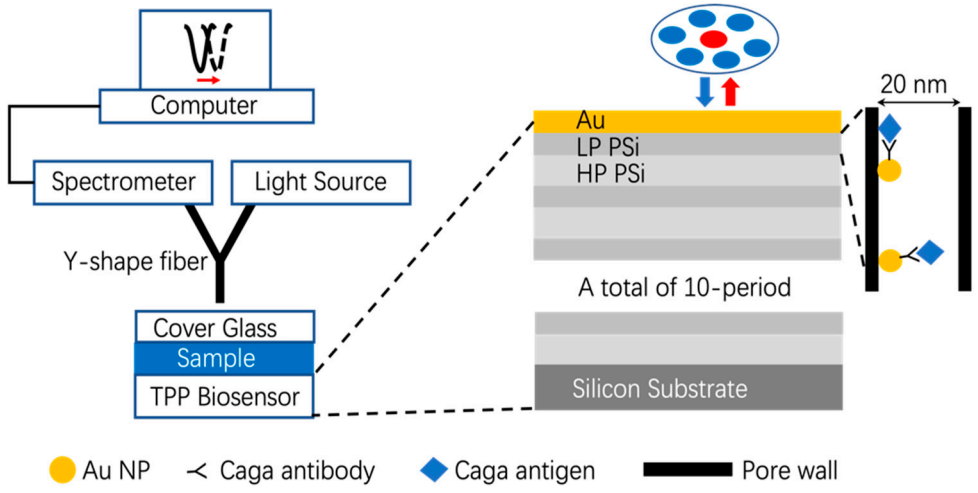

Figure 1. PSi TPP biosensor structure and its optical measurement configuration.

For correction of background noise due to ambient lighting, the light source was turned off and the reflection spectrum was collected of the PSi TPP biosensor which is denoted as $I_{BK}(\lambda)$. Then the actual reflection spectrum of the PSi TPP biosensor after light source and background corrections is:

$$I_{Correct}(\lambda) = \frac{I_{Original}(\lambda) - I_{BK}(\lambda)}{I_{Silver}(\lambda) - I_{BK}(\lambda)} \quad (1)$$

The calculation shown in Eq. (1) is carried out automatically by spectral analysis software during each spectrum measurement. The working principles of the PSi TPP biosensor is as follows. Biomolecules binding inside nanopores of the first porous silicon layer can interact with strongly confined electrical field of the TPP resonant mode. This electrical field is due to the coupling of incident light, an electromagnetic wave with energy inversely proportional to the TPP resonant wavelength, into the TPP resonant mode [28]. This coupling between biomolecules and the electrical field results in perturbation of the electrical field distribution pattern of the TPP resonance mode and will manifest itself as a shift of the TPP resonance wavelength towards longer wavelength in its reflection spectrum [26].

The shift to longer wavelength is also called "redshift" due to the longer wavelength of red light in the visible spectrum. Therefore, the signal processing of TPP biosensor is based on detecting positions of the TPP resonance wavelength in the reflection spectrum collected for both before and

Preprints.org (www.preprints.org) | NOT PEER-REVIEWED | Posted: 31 January 2024 doi:10.20944/preprints202401.2192.v1

after antigen binding in PSi TPP biosensor, and then calculating the shift of the TPP resonance wavelength. More biomolecules binding in PSi TPP biosensor will cause more redshift. This is the mechanism of quantitative detection of biomolecules. Alternatively, there is also machine learning (ML) approach for qualitative determination of detection results for signal and data processing of PSi TPP biosensor [29].

Results and Discussion

Figure 2(a) shows the cross-sectional Scanning Electron Microscopy (SEM) image of the fabricated PSi TPP device. The periodic structure of PSi DBR and the thin gold film on top of DBR are clearly visible. Figure 2(b) shows the simulated electrical field distribution pattern at the resonance wavelength of TPP resonant mode. It can be observed from the colormap that the peak of electrical field resides in the first PSi layer. This PSi layer is also a nanocomposite layer wherein Au nanoparticles generated during sputtering process can infiltrate into porous silicon pores and immobilize on the pore walls [28]. In turn, CagA antigen molecules can also infiltrate into PSi pores and bind with antibodies specifically. Figure 2(c) shows an example of the measured reflection spectrum of the PSi TPP device. The resonance dip shows TPP resonance where light energy at the resonant wavelength is coupled into TPP resonant mode and strong electrical field confinement appears in the proximity to the Au-PSi interface. Figure 2(d) shows an example of the redshift of TPP resonance upon specific binding of CagA antigen with antibodies immobilized on PSi TPP biosensor beforehand. The binding of antigens interacts with locally confined electrical field of TPP resonance. As a result of this perturbation of the TPP mode, the TPP resonance wavelength shifts towards longer wavelengths.

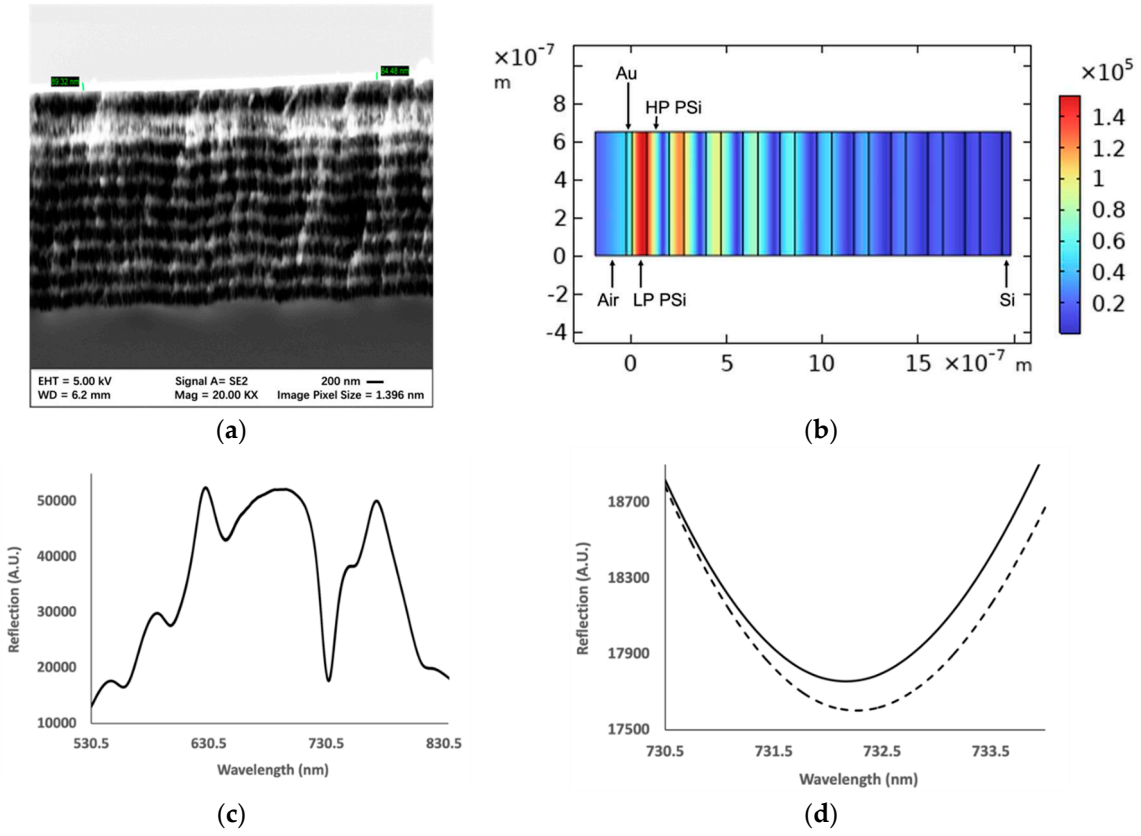

Figure 2. (a) Cross-sectional Scanning Electron Microscopy image of the TPP biosensor structure. The periodic layered structure of the porous silicon DBR is clearly visible. The gold thin film is the bright layer on top of the porous silicon DBR with the thickness not to scale due to a focusing issue; (b) Color map of electrical field strength distribution profile of TPP biosensor. The field peak resides in the first (or top) PSi layer close to the thin metal film. Light is incident from the left side of the TPP device in air with power of 1W/m; (c) An example of the reflection spectrum of TPP device where the resonant

Preprints.org (www.preprints.org) | NOT PEER-REVIEWED | Posted: 31 January 2024 doi:10.20944/preprints202401.2192.v1

state is manifested as the reflection minimum at the wavelength of around 730 nm; (d) Example redshift of the TPP resonance wavelength upon specific biomolecular binding of 3 ng/ml CagA antigen with CagA antibody immobilized on the biosensor surface beforehand. The spectrum of TPP biosensor for both before (solid curve) and after (dashed curve) binding is shown. The shift of resonance minimum towards longer wavelengths is around 360 pm.

To characterize the response of the PSi TPP biosensor, CagA antigen of different concentrations were detected with the PSi TPP biosensor. The redshift vs. antigen concentration can be plotted and the data can be fitted with linear trend. Figure 3 shows the response curve of the PSi TPP biosensor for detecting varying concentration of CagA antigen. A high-quality linear fitting is also given to match the data points at different concentrations. The sensitivity of the PSi TPP biosensor can be defined as:

$$S_{TPP} = \frac{d\lambda_{Res}}{dC} \quad (2)$$

where S_{TPP} is the sensitivity of the PSi TPP biosensor in nm/(ng/ml), λ_{Res} is the TPP resonance wavelength in nm, C is the CagA antigen concentration in ng/ml. The response curve of the PSi TPP biosensor, which is the redshift of TPP resonance wavelength vs. CagA antigen concentration, can be considered as a linear response. From linear fitting of the experimental data obtained at different antigen concentrations, the sensitivity, which is the slope of the fitted curve according to Eq. (2), is 100 pm/ng/ml. Given that the high-resolution spectrometer has a wavelength shift resolution of $\Delta\lambda_{min} = 1\ pm$, the limit of detection can be calculated to be:

$$LOD = \frac{\Delta\lambda_{min}}{S_{TPP}} = 0.01\ ng/ml \quad (3)$$

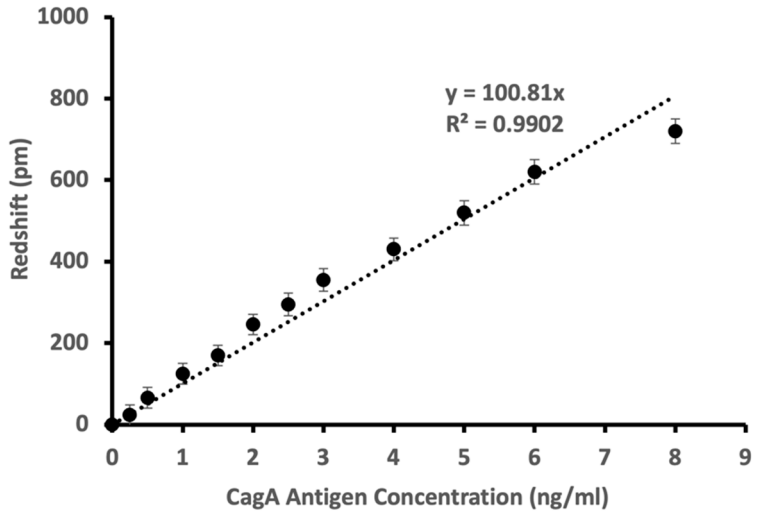

Figure 3. Response characterization of CagA antigen detection for detecting varying concentration of CagA antigen in PBS buffer. Error bars on experimental data points (solid circle) show a standard error from five experiments. The linear fitting (dashed curve) is done to match the data points. The linear equation goes through the origin and the quality of fitting is also given in this figure.

The linear range of the biosensor for CagA antigen detection is 0.25-8 ng/ml, which coincides with the range of CagA antigen concentration in clinical stool specimens [32]. For specificity test of the PSi TPP biosensor, BabA, VacA antigens, BSA (Bovine Serum Albumin), as well as PBS buffer, were used as nonspecific targets of detection. For introduction of interference, BabA antigen and VacA antigen of H. Pylori, and BSA all have concentration of 5 ng/ml, and CagA antigen has concentration of 1 ng/ml. Figure 4 shows the comparison of the specific response signal (the redshift for CagA antigen) with a nonspecific response signal (the redshift for other targets).

Preprints.org (www.preprints.org) | NOT PEER-REVIEWED | Posted: 31 January 2024 doi:10.20944/preprints202401.2192.v1

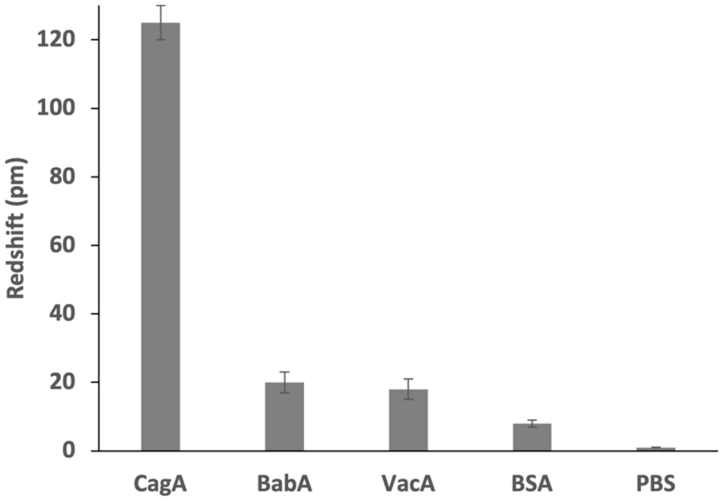

Figure 4. Specificity test of PSi TPP biosensor towards CagA antigen detection. Error bars on experimental data bars (solid rectangle) show standard error from five experiments.

The specific response signal is at least six times stronger than the nonspecific response signal in term of redshift amplitude. This demonstrates the good specificity of the PSi TPP biosensor towards detection of CagA antigen of H. Pylori. To compare our proposed PSi TPP biosensor with biosensors reported in literature, Table 4 shows a comparison of the performances of PSi TPP biosensor with other state-of-the-art biosensors for detection of CagA antigen/antibody. It demonstrates that the PSi TPP biosensor has superior performance and is competitive for application in onsite rapid diagnosis of H. Pylori infection.

Table 4. Comparison of Biosensing Performances of CagA antigen/antibody detection for H. Pylori diagnosis.

Biosensor Technique	Sensitivity	LOD (ng/ml)	Linear Range (ng/ml)	Positive-to-Negative Ratio
Amperometric [32]	656.0 μA/(ng/ml)	0.10	0.1-8	>5
Electrochemical [33]	0.275 μA/(ng/ml)	0.05	0.05-50	~4
Voltametric [34]	1.0 μA/(ng/ml)	0.20	0.2-50	>5
TPP (This work)	100 pm/(ng/ml)	0.01	0.25-8	>6

Conclusion

In this original research work, we have developed and demonstrated for the first time, to the best of our knowledge, a high-performance porous silicon Tamm Plasmon Polariton optical biosensor for the detection of CagA antigen of H. Pylori bacterium with application in the diagnosis of H. Pylori infection. The PSi TPP biosensor is composed of porous silicon multilayer structure, which is a Distributed Bragg Reflector, and a plasmonic layer which is gold thin film. These two components comprise the PSi TPP device and the optical biosensor thereafter. After optimization in biosensor design, fabrication and biofunctionalization, the sensitivity of the PSi TPP biosensor can be up to 100 pm/(ng/ml), and the limit of detection can be down to 0.01 ng/ml. In addition, the good specificity of the PSi TPP biosensor is demonstrated by the positive-to-negative ratio of more than a factor of six.

Preprints.org (www.preprints.org) | NOT PEER-REVIEWED | Posted: 31 January 2024 doi:10.20944/preprints202401.2192.v1

These experimental results demonstrate the characteristics of the PSi TPP biosensor for CagA antigen detection and therefore its suitability for H. Pylori infection diagnosis.

There are a lot of future research opportunities concerning PSi TPP biosensor. These ranges from structural optimization and material selection for improvement of sensitivity, to clinical experiments for practical applications. Researchers can carry out further optimization of the PSi TPP biosensor by incorporating tunable epsilon-near-zero material, such as graphene, into the TPP device structure to replace noble metal material [35]. Graphene has the property of tunable conductivity, thus allowing the tuning of the TPP resonance wavelength and the electrical field confinement profile of the TPP resonant mode. Also, Optical Tamm State (OTS) [36], which can be confined at the interface between two symmetric or asymmetric photonic crystals, can couple with TPP resonant mode and the resulting Fano resonance [37] can have tunable field confinement profile depending on the coupling strength between OTS and TPP modes. Moreover, the flexibility in the design of DBR structure, such as design of aperiodic DBR [38], can allow for better quality factor of the TPP resonance and more space for field confinement optimization. In addition, due to the compatibility of porous silicon fabrication with CMOS processes, integration of PSi TPP biosensor with silicon-based optoelectronics and electronics is also interesting in terms of lowering cost, reducing the form factor of the whole system, improving reliability and repeatability, and promoting clinical applications. For clinical use, experimental detection of real clinical specimens, such as stool of patients, need to be done to characterize the performance of the PSi TPP biosensor in complex specimens containing various kinds of bio species.

In summary, optical biosensor based on PSi TPP is an attractive biosensing technology for detecting pathogens and their related antigens. It has vast potential for rapid onsite detection required in scenarios such as population screening, epidemic surveillance, and personal healthcare. Well poised to act as an onsite rapid diagnostic tool for POCT applications, PSi TPP biosensor can serve as an indispensable complement to central analytical lab-based detection techniques such as PCR and sequencing. Therefore, PSi TPP biosensor can be an efficient platform to curb pathogen dissemination and help improve healthcare outcomes.

Author Contributions: Conceptualization, G.R., A.K. and M.S.; methodology, G.R., A.K. and M.S.; software, G.R.; writing—original draft preparation, G.R.; writing—review and editing, A.K. and M.S.; supervision, M.S.; funding acquisition, M.S. All authors have read and agreed to the published version of the manuscript.

Funding: This research was funded by the Leading Innovative and Entrepreneur Team Introduction Program of Zhejiang grant number 2020R01005, Westlake University grant number 10318A992001, Tencent Foundation grant number XHTX202003001, and Zhejiang Key R&D Pro-gram grant number 2021C03002. The APC was funded by the Leading Innovative and Entrepreneur Team Introduction Program of Zhejiang.

Institutional Review Board Statement: Not applicable.

Informed Consent Statement: Not applicable.

Data Availability Statement: The data presented in this study are available on request from the corresponding author. The data are not publicly available due to privacy.

Conflicts of Interest: The authors declare no conflict of interest.

References

1. Leja, M., A. Axon, and H. Brenner, *Epidemiology of Helicobacter pylori infection.* Helicobacter, 2016. **21**: p. 3-7.
2. de Brito, B.B., et al., *Pathogenesis and clinical management of Helicobacter pylori gastric infection.* World Journal of Gastroenterology, 2019. **25**(37): p. 5578-5589.
3. Sun, Q.F., et al., Helicobacter pylori infection: a dynamic process from diagnosis to treatment. Frontiers in Cellular and Infection Microbiology, 2023. **13**.

Preprints.org (www.preprints.org) | NOT PEER-REVIEWED | Posted: 31 January 2024 doi:10.20944/preprints202401.2192.v1

4. Malfertheiner, P., et al., Management of infection: the Maastricht VI/Florence consensus report. Gut, 2022. **71**(9): p. 1724-1762.
5. Llorca, L., et al., Comparative, Prospective, Study Comparing the Accuracy of Two Different Stool Antigen Tests (Premier Platinum Hpsa and Novel Immunocard Stat! Rapid Test) for the Diagnosis of Infection: Preliminary Results. Helicobacter, 2015. **20**: p. 88-88.
6. Su, X.D. and S.F.Y. Li, Serological determination of infection using sandwiched and enzymatically amplified piezoelectric biosensor. Analytica Chimica Acta, 2001. **429**(1): p. 27-36.
7. Ly, S.Y., H.S. Yoo, and S.H. Choa, *Diagnosis of bacterial infections using a voltammetric biosensor.* Journal of Microbiological Methods, 2011. **87**(1): p. 44-48.
8. Shahrashoob, M., et al., Detection of Genome with an Optical Biosensor Based on Hybridization of Urease Gene with a Gold Nanoparticles-Labeled Probe. Journal of Applied Spectroscopy, 2016. **83**(2): p. 322-329.
9. Sezgin, G.C. and I. Ocsoy, Anthocyanin-rich black carrot (ssp. sativus var. atrorubens Alef.) and red cabbage () extracts incorporated biosensor for colorimetric detection of with color image processing. Brazilian Journal of Microbiology, 2023. **54**(2): p. 897-905.
10. Ono, S., et al., Accuracies of Endoscopic Diagnosis of Gastritis: Multicenter Prospective Study Using White Light Imaging and Linked Color Imaging. Digestion, 2020. **101**(5): p. 624-630.
11. Akeel, M., et al., Efficacy of immunohistochemical staining in detecting in Saudi patients with minimal and atypical infection. European Journal of Histochemistry, 2021. **65**(3).
12. Malfertheiner, P., et al., Management of infection-the Maastricht IV/ Florence Consensus Report. Gut, 2012. **61**(5): p. 646-664.
13. Wong, A., S.S. Ching, and A.S. Long, The use of a second biopsy from the gastric body for the detection of using rapid urease test. Singapore Medical Journal, 2014. **55**(12): p. 644-647.
14. Bénéjat, L., et al., Real-time PCR for diagnosis. The best tools available. Helicobacter, 2018. **23**(5).
15. Rong, G., et al., *Nanoscale porous silicon waveguide for label-free DNA sensing.* Biosensors & Bioelectronics, 2008. **23**(10): p. 1572-1576.
16. Verma, Y.K., S. Kumari, and S.M. Tripathi, *Grating assisted temperature insensitive micro-ring resonator biosensor.* Journal of Optics, 2023. **25**(12).
17. Wu, B., et al., A Nanoscale Porous Silicon Microcavity Biosensor for Novel Label-Free Tuberculosis Antigen-Antibody Detection. Nano, 2012. **7**(6).
18. Nagarathnegowda, M., et al., A Gallium arsenide composite semi-conductive material-based 2D photonic crystal biosensor for cancer cell detection. Optical and Quantum Electronics, 2023. **55**(12).
19. Esmailidastjerdipour, P. and F. Shahshahani, Numerical Simulation of Fiber Optic Biosensor Consisting of Metal/ScO Enhancing by Using Aluminum Alloy for Hydrotherapy Applications. Plasmonics, 2023.
20. Das, C.M., et al., Computational Modeling for Intelligent Surface Plasmon Resonance Sensor Design and Experimental Schemes for Real-Time Plasmonic Biosensing: A Review. Advanced Theory and Simulations, 2023. **6**(9).
21. Semwal, V., et al., Investigation of Performance Parameters of Spherical Gold Nanoparticles in Localized Surface Plasmon Resonance Biosensing. Micromachines, 2023. **14**(9).
22. Tripathi, M.N., et al., A novel approach for rapid and sensitive detection of Zika virus utilizing silver nanoislands as SERS platform. Spectrochimica Acta Part a-Molecular and Biomolecular Spectroscopy, 2023. **302**.
23. Wan, Y.H., et al., Resonant Mode Engineering of Photonic Crystal Sensors Clad with Ultralow Refractive Index Porous Silicon Dioxide. Advanced Optical Materials, 2017. **5**(21).
24. Rong, G.G., et al., A high-throughput fully automatic biosensing platform for efficient COVID-19 detection. Biosensors & Bioelectronics, 2023. **220**.
25. Rong, G.G., et al., A Closed-Loop Approach to Fight Coronavirus: Early Detection and Subsequent Treatment. Biosensors-Basel, 2022. **12**(10).
26. Rong, G.G. and M. Sawan, Tamm Plasmon Polariton Biosensors Based on Porous Silicon: Design, Validation and Analysis. Biosensors-Basel, 2023. **13**(12).
27. Kaliteevski, M., et al., Tamm plasmon-polaritons: Possible electromagnetic states at the interface of a metal and a dielectric Bragg mirror. Physical Review B, 2007. **76**(16).
28. Vyunishev, A.M., et al., *Broadband Tamm plasmon polariton.* Journal of the Optical Society of America B-Optical Physics, 2019. **36**(8): p. 2299-2305.
29. Rong, G.G., Y.K. Xu, and M. Sawan, Machine Learning Techniques for Effective Pathogen Detection Based on Resonant Biosensors. Biosensors-Basel, 2023. **13**(9).
30. Umit, H., et al., The Relationship Between Virulence Factors of Helicobacter pylori and Severity of Gastritis in Infected Patients. Digestive Diseases and Sciences, 2009. **54**(1): p. 103-110.
31. Ni, H.K., et al., The relationship between gastric cancer and Helicobacter pylori cytotoxin-related gene A genotypes. Cellular and Molecular Biology, 2020. **66**(7): p. 1-4.
32. Jain, U., et al., Triple-nanostructuring-based noninvasive electro-immune sensing of CagA toxin for detection. Helicobacter, 2020. **25**(4).

Preprints.org (www.preprints.org) | NOT PEER-REVIEWED | Posted: 31 January 2024 doi:10.20944/preprints202401.2192.v1

33. Saxena, K., et al., Fabrication of a Molecularly Imprinted Nano-Interface-Based Electrochemical Biosensor for the Detection of CagA Virulence Factors of. Biosensors-Basel, 2022. **12**(12).
34. Chauhan, N., et al., *Zinc Oxide Tetrapods Based Biohybrid Interface for Voltammetric Sensing of.* Acs Applied Materials & Interfaces, 2018. **10**(36): p. 30631-30639.
35. Kumar, M. and S. Prasad, High-Resolution Temperature Sensor Based on Resonance Excitation of Tamm Plasmon Polaritons: Graphene Plasmon Polariton Hybrid Mode. Journal of Electronic Materials, 2023. **52**(8): p. 5337-5344.
36. Wu, F., et al., Broadband wide-angle multilayer absorber based on a broadband omnidirectional optical Tamm state. Optics Express, 2021. **29**(15): p. 23976-23987.
37. Wang, Z.Y., et al., High and Tailorable Fano Resonances in a One-Dimensional Metal-Optical Tamm State Structure: From a Narrowband Perfect Absorber to a Narrowband Perfect Reflector. Advanced Functional Materials, 2021. **31**(26).
38. He, M.Z., et al., Deterministic inverse design of Tamm plasmon thermal emitters with multi-resonant control. Nature Materials, 2021. **20**(12): p. 1663-+.

Disclaimer/Publisher's Note: The statements, opinions and data contained in all publications are solely those of the individual author(s) and contributor(s) and not of MDPI and/or the editor(s). MDPI and/or the editor(s) disclaim responsibility for any injury to people or property resulting from any ideas, methods, instructions or products referred to in the content.